Z. Phys. C 63, 409–416 (1994)

ZEITSCHRIFT
FÜR PHYSIK C

A new experimental limit on neutron-antineutron oscillations

M. Baldo-Ceolin[3], P. Benetti[4], T. Bitter[1], F. Bobisut[3], E. Calligarich[4], R. Dolfini[4], D. Dubbers[1], P. El-Muzeini[1], M. Genoni[4], D. Gibin[3], A. Gigli Berzolari[4], K. Gobrecht[2], A. Guglielmi[2], J. Last[2], M. Laveder[3], W. Lippert[1], F. Mattioli[3], F. Mauri[4], M. Mezzetto[3], C. Montanari[4], A. Piazzoli[4], G. Puglierin[3], A. Rappoldi[4], G.L. Raselli[4], D. Scannicchio[4], A. Sconza[3], M. Vascon[3], L. Visentin[3]

[1] Physikalisches Institut, University of Heidelberg, D-69120 Heidelberg, Germany
[2] Institut Max von Laue-Paul Langevin (ILL), Grenoble, France
[3] Dipartimento di Fisica "G. Galilei", University of Padova and I.N.F.N. Sezione di Padova, Padova, Italy
[4] Dipartimento di Fisica Nucleare e Teorica, University of Pavia and I.N.F.N. Sezione di Pavia, Pavia, Italy

Received: 28 February 1994

Abstract. The experimental search for neutron-antineutron oscillations has been completed at the ILL high flux reactor at Grenoble. A neutron beam of intensity 10^{11} n s^{-1} was propagated for a time $t \simeq 0.1$ s in vacuum in a region shielded against the external magnetic field. No antineutron was detected in $2.4 \cdot 10^7$ s running time. The lower limit $\tau_{n\bar{n}} \geqq 0.86 \cdot 10^8$ s for $n\bar{n}$ transitions was established at 90% C.L.

1 Introduction

Baryon number non conserving interactions with $\Delta B = 2$, $\Delta L = 0$ may induce $n \rightleftharpoons \bar{n}$ mixing and consequently $n \rightleftharpoons \bar{n}$ oscillations, which could take place via a first order process, and are characterized by an oscillation time $\tau_{n\bar{n}}$. Then, provided new physics occurs beyond the Standard Model at the mass scale of the order of 10^2 to 10^3 TeV the oscillation time $\tau_{n\bar{n}}$ could be in the region of 10^8 s [1]. The experiment described in this paper was designed to detect $n \rightleftharpoons \bar{n}$ oscillations occurring in times less than $\sim 10^8$ s. A preliminary result, giving a lower limit of $\tau_{n\bar{n}} \geqq 10^7$ s at the 90% C.L., has already been published by this collaboration [2]. Limits at the 90% C.L. $\tau_{n\bar{n}} \geqq 10^6$ s [3] and $\tau_{n\bar{n}} \geqq 0.5 \cdot 10^6$ s [4] were reached in two previous experiments performed with free neutron beams. In addition, underground proton decay type experiments, through measurements of nuclear lifetime, were able to set the lower limit $\tau_{n\bar{n}} > 10^8$ s [5]. It was made clear however that the evaluation of $\tau_{n\bar{n}}$ from this type of measurements rests on nuclear model assumptions [6]. Moreover it was stressed that, since the strength of the $n \rightleftharpoons \bar{n}$ transitions needs not be the same for free neutrons or neutrons bound in nuclear matter [7], the only model independent measurement of $\tau_{n\bar{n}}$ can come from experiments on free neutrons.

In the hypothesis of $n \rightleftharpoons \bar{n}$ oscillations, the probability of generating antineutrons after a time t, $P(\bar{n}, t)$, in a state which was initially composed only of neutrons, is expressed by the equation

$$P(\bar{n}, t) = \frac{\delta m^2}{\delta m^2 + \Delta E^2} \sin^2 \left(\sqrt{\delta m^2 + \Delta E^2} \cdot t\right), \tag{1}$$

where $\delta m = (\tau_{n\bar{n}})^{-1} \leqq 6 \cdot 10^{-29}$ MeV is the $n \rightleftharpoons \bar{n}$ transition energy, and ΔE is half of the energy gap between the n and $\bar{n}$ states due to external field perturbations, either nuclear or electromagnetic.

For neutrons bound in nuclei $(\Delta E_N) \approx 100$ MeV and, according to (1), the $n \rightleftharpoons \bar{n}$ oscillation amplitude, $(\delta m / \Delta E_N)^2$, is smaller than 10^{-60}. Moreover, also in the case of artificially produced unbound neutrons, propagating in vacuum where (ΔE_N) is equal to zero, a magnetic field B, acting along the neutron propagation path, would give rise to a $(\Delta E_B) = \mu B$, since n and $\bar{n}$ have equal but opposite sign magnetic moments: $|\mu| = 6 \cdot 10^{-14}$ MeV $\cdot T^{-1}$.

The Earth's magnetic field for instance would produce $(\Delta E_B) \approx 10^{-18}$ MeV and reduce the oscillation amplitude of neutrons propagating in vacuum to $(\delta m / \Delta E_B)^2 < 10^{-22}$, still a very small value.

On the contrary, in the ideal case, where neutrons propagate in the absence of perturbing fields, $\Delta E = 0$ and the $n \rightleftharpoons \bar{n}$ transition probability (1) becomes

$$P(\bar{n}, t) = \sin^2 (\delta m\, t). \tag{2}$$

In this case for $t \ll \tau_{n\bar{n}}$, the antineutron component increases proportionally

$$P(\bar{n}, t) \simeq \left(\frac{t}{\tau_{n\bar{n}}}\right)^2. \tag{3}$$

An important feature of an $N\bar{N}$ experiment with unbound neutrons consists in the fact that (3) properly describes the time evolution of the $\bar{n}$ component, provided that external field perturbations are reduced to such a level that

$$\Delta E \cdot t \ll 1. \tag{4}$$

Condition (4) is defined as the *quasi free condition* [8]. In numbers, for a propagation time $t \simeq 0.1$ s, the requirement of (4) can be fulfilled if the residual pressure and the magnetic field along the neutron propagation region are reduced to $P < 10^{-2}$ Pa and $B < 10$ nT respectively.

Once condition (4) is satisfied, (1) can be more simply expressed in terms of the experimental parameters as follows:

$$\frac{\bar{N}}{\varepsilon} = IT\left(\frac{1}{\tau_{n\bar{n}}}\right)^2\left(\frac{L}{v}\right)^2, \tag{5}$$

where $\frac{\bar{N}}{\varepsilon}$ is the number of antineutrons, ε is the antineutron detection efficiency, I is the neutron intensity, T the running time, L the propagation region length and v the neutron velocity. From (5) it appears that experiments searching for $n \rightleftharpoons \bar{n}$ transitons with free neutrons, require a very high flux source of low neutrons, a long and well shielded propagation region, a properly designed target, where antineutrons eventually annihilate, and a detector covering a large solid angle with good energy and space resolutions to identify annihilation events.

The experiment described in the following was designed to measure $n \rightleftharpoons \bar{n}$ oscillation times up to 10^8 s. It made use of a total of $3 \cdot 10^{18}$ neutrons with an average velocity $v \approx 600\ \mathrm{m\,s^{-1}}$ propagated for a time $t \simeq 0.1$ s in a region where residual pressure and magnetic field were maintained at the values required by the *quasi free condition.* The final antineutron detection efficiency was $\varepsilon \simeq 0.5$. No antineutrons were detected during the experiment, which gave a limit of

$$\tau_{n\bar{n}} \geqq 0.86 \cdot 10^8\ \mathrm{s}, \tag{6}$$

at 90% C.L.

2 Experimental set-up

The most sensitive parameters for the experimental sensitivity were the neutron source intensity, the quasi free propagation time, and the $\bar{n}$ detection efficiency.

The experiment was carried out at the 58 MW high flux reactor (HFR) at the Institute Laue-Langevin (ILL) in Grenoble, where intense source of slow neutrons were available. Figure 1 shows a sketch of the experimental set-up, which was previously described in [2].

The main parameters in the experiment were chosen to be $I > 10^{11}\ \mathrm{n\,s^{-1}}$, the total running time $T \simeq 1$ year, $t > 0.1$ s, and $\varepsilon > 0.7$.

The most severe constraints were the associated beam noise and the cosmic ray background.

2.1 Neutron source

Neutrons from the HFR were moderated to liquid D_2 temperature (25 K) at the Horizontal Cold Source and transported to the experimental area through a system of neutron guides [9]. An important characteristic of the neutron guides is their ability to propagate intense neutron beams over long distances, while maintaining the neutron beam intensity, cross-section and divergence with respect to the beam axis, practically constant. The $N\bar{N}$ experiment was fed through the H53 line, a system of totally reflecting neutron guides, ^{58}Ni coated, 63 m long, $6 \times 12\ \mathrm{cm^2}$ cross-section. The neutron guides were slightly bent in order to eliminate γ's and fast neutrons coming directly from the reactor. The H53 neutron intensity was measured to be $I_0 \simeq 1.7 \cdot 10^{11}\ \mathrm{n\,s^{-1}}$ [10]. Figure 2 shows the neutron energy spectrum and angular divergence as a function of their wavelength λ. The neutron average wavelength was $\lambda \simeq 6.5$ Å corresponding to an energy of $2 \cdot 10^{-3}$ eV and a velocity of $600\ \mathrm{m\,s^{-1}}$. The average angular divergence with respect to the beam axis was 5.7 mrad, varying from 0 up to 40 mrad.

The $N\bar{N}$ experiment initiated 4 m downstream from the exit of H53, where neutrons were transported by means of neutron guides and traversed an apparatus

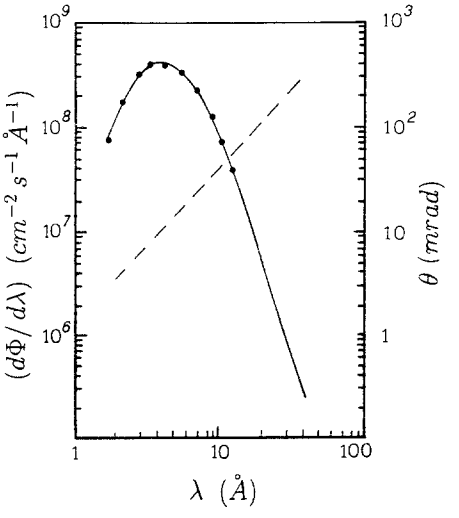

Fig. 2. The neutron beam spectrum (full line) and the maximum neutron angular divergence (dashed line) as a function of the neutron wavelength λ

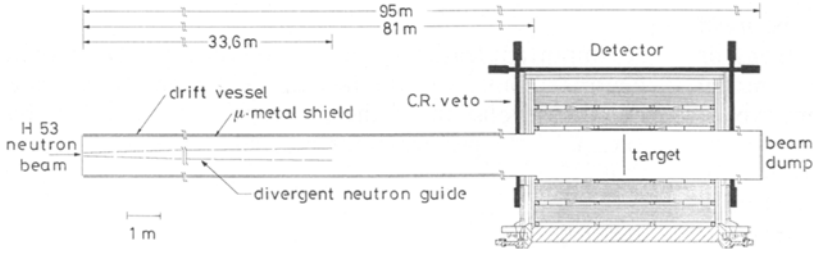

Fig. 1. The $N\bar{N}$ experimental set-up

(EVA) located in between. A sizeable part of the beam (22%) was lost on the way. At the entrance of the $N\bar{N}$ beam line the neutron intensity was measured to be $I_0 \simeq 1.3 \cdot 10^{11}\ \mathrm{n\,s^{-1}}$; the beam properties, energy and divergence distributions, were measured to be practically unchanged after the exit of H53.

2.2 *Neutron propagation region*

A propagation region was set up where neutrons could propagate for a time $t \simeq 0.1$ s under the *quasi free condition* aiming at a sensitivity $\tau_{n\bar{n}} \simeq 10^8$ s in about 1 year running time. The drift vessel had to be carefully designed for the containment of the whole neutron beam, otherwise the radiation coming from neutron captures on the walls would have produced an intolerable noise in the detector.

The H53 neutron divergence would have implied a beam cross-section at the detector several square meters large. Therefore, aiming at constraining within 1 m^2 the neutron beam cross-section at the target, a system was devised which consisted of a straight beam guide with slightly divergent walls. With this device the neutron divergence was reduced after each reflection by 2δ, δ being the guide wall divergence [11]. The parameters of the divergent guide were devised with a Monte Carlo (MC) program which was developed taking into account the neutron energy and divergence distributions. A straight divergent guide system was constructed, which, according to the needs, was able to decrease the neutron divergence by a factor of 2.7 on average (Fig. 3). It consisted of 33 reflecting elements, coated with natural nickel. Each element, 1 m long, with the walls at an angle $\delta = 3$ mrad with respect to the beam axis, was separated by 2 cm from the next one [10].

The drift vessel consisted of three contiguous parts: the oscillation region, the annihilation region and the beam dump. The first part, the oscillation region, was a stainless steel drift vessel 81 m long, 1.2 m diameter, 0.5 cm thick. The divergent guide was installed inside the drift vessel at the neutron entrance. Moreover, a passive μ metal shield was installed coaxially inside the drift vessel (see Fig. 1), in order to shield the oscillation region from the earth's magnetic field as well as from any other stray field. The second part of the drift vessel, the annihilation region, was an Al tube 5.6 m long, 1.4 m diameter and 0.8 cm thick. The antineutron annihilation target previously used in experiment [4] consisted of a carbon foil 130 μm thick and 110 cm diameter, suspended in the central part of the annihilation region. The distance from the outer edge of the target to the wall was 15 cm; a MC study on the separation between events on the wall and those on the target dictated this dimension. The main characteristics of the target were: an annihilation probability for $\bar{n}$ larger than 99% [12]; a low Z to preserve the peculiar features of the annihilation events; a high transparency to the neutron beam and a mass of ~ 180 g. Neutrons scattered by the target were absorbed by a ^{6}LiF layer, 2 mm thick and 5 m long, overlaying the inner wall of the annihilation region [13].

A 2.5 cm thick stainless steel disk, covered with a 0.4 cm thick layer of ^{6}LiF, acted as an efficient neutron beam dump. It closed the third part of the drift vessel, a stainless steel tube 7.8 m long, 0.5 cm thick, with the same cross-section as the annihilation region.

The neutron propagation region was about 100 m long, and the neutron trajectories were bent downward by gravity. In order to compensate for this vertical displacement, the drift vessel was lowered with respect to the beam axis by 6.7 cm in the first part and 9 cm in the rest. Even so, a small part of the neutron beam impinged on the walls. In order to minimize the noise produced at the detector by these stray neutrons, eight rings of boron enriched glass were installed inside the drift vessel at different distances along the oscillation region, as was indicated by a detailed MC study.

Measurements showed that only a very small fraction of the incoming neutron beam (2.5%) was lost along the divergent neutron guide. A further small fraction (2.7%) was lost along the drift vessel, after the divergent guide, due to the vertical fall of the free neutrons. Most of these neutrons were absorbed by the boron, producing a practically negligible noise level at the detector. The neutron beam intensity measurements performed by gold foil activation in several positions along the beam line, gave a result in very good agreement with the MC calculations [14, 10].

The neutron intensity at the target was measured to be $I \simeq 1.25 \cdot 10^{11}\ \mathrm{s^{-1}}$. It was found that, as an effect of the neutron transportation system, the neutron energy spectrum was slightly depleted in the lower energy component, so that the average wavelength became $\lambda = 5.9$ Å. The full neutron beam was contained in the target, but a 10^{-3} fraction which flew directly to the beam dump.

During the experiment 3 neutron counters, inserted in the ^{6}LiF beam dump, provided continuous monitoring of the beam intensity and shape.

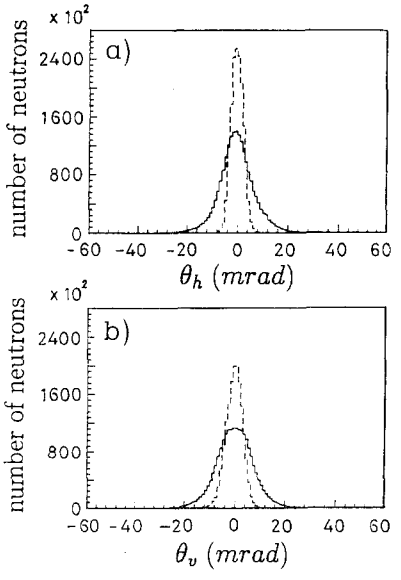

Fig. 3a, b. The distribution of the horizontal **a** and vertical **b** neutron angular divergence at the entrance (full line) and at the exit (dashed line) of the neutron divergent guide

2.3 The quasi free condition

The free neutron propagation time was evaluated with a MC calculation where all the general features of the neutron beam as well as those of the propagation region were taken into account. For each neutron the distance from its last reflection on the divergent guide to the exit from the shielded region was taken to be the length of the free propagation. The effective time for neutron oscillation then became

$$\langle t^2\rangle^{1/2}=\left(\frac{1}{I}\cdot\int \mathrm{d}t\,\frac{\mathrm{d}I}{\mathrm{d}t}\cdot t^2\right)^2=(0.109\pm 0.002)\,\mathrm{s}\,, \tag{7}$$

and the $\bar{n}$ probability distribution on the target is shown in Fig. 4 [10]. Then, in order that the quasi free condition be satisfied by the whole neutron beam, the residual pressure was constrained [15] to the value $p_{\mathrm{res}}<10^{-2}$ Pa, under the assumption that a) $\Delta E_{\mathrm{gas}}=\pi N\hbar^2 m^{-1}\times(f-\bar{f})\ll 10^{-23}$ MeV, where m is the n mass, N is the number density of scatterers and f, $\bar{f}$ are the mean forward amplitudes for n an $\bar{n}$; b) the probability that antineutrons, eventually produced by $n\rightleftharpoons\bar{n}$ transitions, annihilate before reaching the target be less than 1%. During the experiment two turbomolecular pumps maintained $p_{\mathrm{res}}\simeq 2\cdot 10^{-4}$ Pa in the whole drift vessel.

The oscillation region moreover had to be shielded against the Earth's magnetic field as well as from any other stray field. The Earth's magnetic field in Grenoble was measured to be $B\simeq 5\cdot 10^{-5}$ T, in which case the quasi free condition required a suppression of B of the order of 10^{-3}. A MC calculation, taking into account the neutron energy distribution, had shown that a residual $B=10$ nT along the neutron beam oscillation region satisfied the quasi free condition at the 99% level. A residual magnetic field $B<10$ nT was obtained by means of a passive μ-metal shield plus an active system providing field compensating currents. The μ-metal shield, 76 m long, 1.1 m diameter and 1 mm thick, installed coaxially inside the propagation region, gave an excellent suppression of the transverse component by a factor $\simeq 2000$. However it was not effective for the axial field, which was compensated by a 80 m long solenoid wound around the vacuum tube. The residual magnetic field was measured to be $B<10$ nT everywhere but on the μ-metal junctions where it presented a sudden short variation.

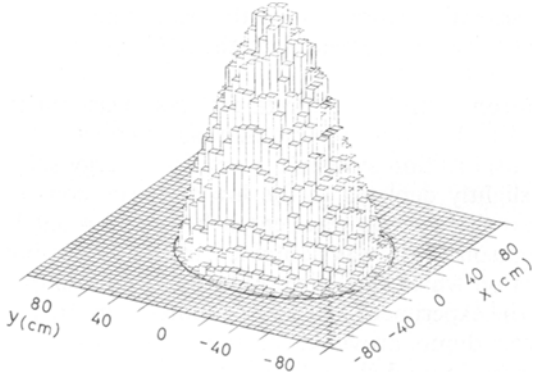

Fig. 4. The expected $\bar{n}$ distribution on the target

This effect was carefully taken into account in the analysis [16, 17], where the efficiency for the quasi free condition was given by the parameter

$$\eta=\frac{P(\bar{n},t,B)}{P(\bar{n},t,B=0)}\,. \tag{8}$$

A probe with a sensitivity at the level of nT was installed in a fixed position in the beam tube, monitoring the status of the magnetic field continuously. It gave the feedback to the active shield and checked for anomalous field conditions. In addition, twice a day a complete map of the magnetic field along the beam was measured. The average η value during the experiment was:

$$\langle\eta\rangle=(0.984\pm 0.003)\,. \tag{9}$$

A very direct global test of the residual magnetic field was also made, using the neutrons themselves, with the "neutron spin magnetometry" method described in [18] and found in excellent agreement with the other measurements.

2.4 The detector

The $\bar{n}$-annihilation detector was a tracking device which consisted of limited streamer tube (LST) planes [19] and scintillation counter (SC) planes (Fig. 5). Organized in four quadrants, it surrounded the target covering a solid angle $\Delta\Omega/4\pi=0.94$. The LST dimensions were $0.9\times 0.9\times 500$ cm^3; they were operated with a three component gas mixture (88% CO_2, 3% Ar, 9% C_4H_{10}) at the voltage of 4.6 kV.

The detector consisted essentially of three parts: a vertex detector, a SC hodoscope and a calorimeter. The vertex detector embodying the target region was the inner part. It was made of 10 LST planes supported by Al honeycomb plates 2 cm thick. The detector average density, $\rho=0.3$ g cm^{-3}, together with the high track sam-

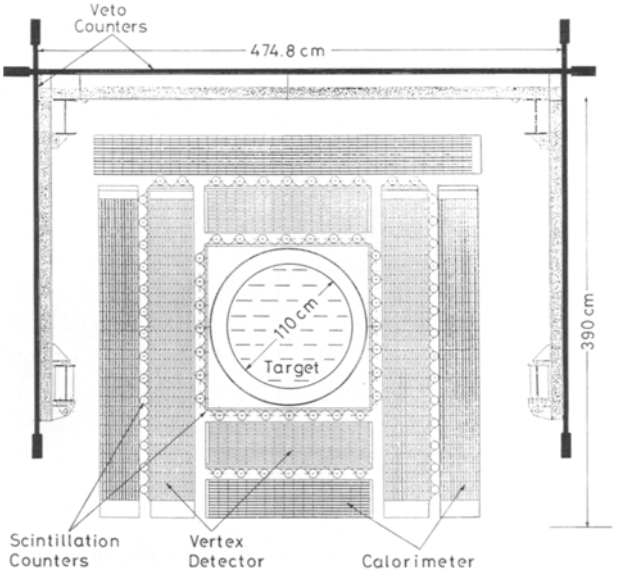

Fig. 5. The $\bar{n}$ annihilation detector (cross sectional view)

pling made it possible to measure the directions of the charged particles produced in the $\bar{n}$-annihilation events.

The purpose of the SC hodoscope was twofold: to provide early and fast signals for the first trigger level via a specially designed mean timer [20], and to measure the time of flight (TOF) of the particles. A layer of SC 2 cm thick, 21 cm large, equipped with light guides and photomultipliers (PMT) at both ends, were placed in front and on the back of the vertex detector. The inner SCs were 210 cm long, the outer ones 300 cm long, and covered a solid angle $\Delta\Omega/4\pi = 0.8$ around the annihilation target. TOF was designed primarily to discriminate particles generated by $\bar{n}$-annihilation events in the target and travelling from the inner to the outer part against particles produced by neutral cosmic rays in the detector and travelling towards the target from the outer to the inner SC. MC simulations of $\bar{n}$-annihilation events (see below) showed that with TOF resolution $\sigma_{TOF} = 700$ ps only 0.2% of the events would have had a particle with a measured TOF of the wrong sign. During the experiment the TOF resolution was measured regularly by selecting cosmic ray (CR) muons crossing the outer and inner SC planes and found $\sigma_{TOF} \sim 600$ ps. To monitor the time accuracy during the runs, very short pulses ($\Delta t = 200$ ps) of laser light illuminated the middle of each counter through a system of optical fibers. Every day the relative timing of all counters was measured and recorded; moreover these timings were also compared with those obtained triggering on CR muons immediately before and after the beam-on periods (~ 44 days long). Both the day by day check and the comparison between laser and CR timings allowed the timing stability at the 150 ps level during the whole experiment [21] to be maintained.

The third part of the detector was a calorimeter. It was placed behind the external scintillator layer and consisted of 12 LST planes alternated with planes made of Pb plates (0.1 cm thick the first six, and 0.2 cm the others) sandwiched between 0.25 cm thick Al plates.

The streamer signals on LST were collected by x and y pickup strips and read out by 32 channels digital cards. More than 60 000 electronic channels were implemented. The read-out control and data compression were carried out by a specially designed CAMAC module (STROC) [22]. The LST system was continuously monitored and the percentage of disconnected streamer tubes never exceeded the 2% level.

An active veto shielding against charged cosmic rays completely overlayed the detector. The CR veto was made of 235 plastic SC covering a total area of 95 m^2. To improve the geometrical veto efficiency as well as to reject CR induced high energy showers produced in the detector, a part of the SC, covering an additional area of 5×4 m^2, was placed below the 80 cm concrete platform supporting the detector. Each veto counter was equipped with two light guides and two PMTs, whose signals, in order to reduce the dead time of the experiment, were processed by mean timers of the type mentioned above. The veto system was continuously monitored and the dead time measured by a dedicated processor [23].

Moreover, to shield the apparatus against neutral CR, a passive veto was placed between the calorimeter and the veto counters, which was also designed to prevent possible autovetoing of $\bar{n}$ annihilation event. It consisted of planes of lead, 10 cm thick, canned into boxes of stainless steel chosen to avoid magnetic field distortions.

3 Trigger and data acquisition

A trigger made of a coincidence of an inner and an outer SC on the same detector quadrant, in anticoincidence with the CR veto counters, was expected to have an efficiency $\varepsilon_{trig} = 0.8$ for $\bar{n}$-annihilation events in the target. However neutron captures in the annihilation target produced an inconveniently high noise in the detector [13]: about 1 MHz of counters in the SC inner shell and ~ 2000 Hz coincidences between the inner and outer SC in the same quadrant. The trigger [24] was then also required to satisfy the following additional conditions:

a) At least one charged track crossing the same vertex detector quadrant in which the SC coincidence occurred. A charged track was defined by a coincidence of signals from at least 4 out of 10 LST planes. This requirement reduced the trigger rate to $\simeq 800$ Hz.
b) At least one SC firing in another quadrant, and in addition at least a second track in the detector, either in the vertex detector or in the calorimeter, reducing the trigger rate to $\simeq 6$ Hz.
c) A total number of hits $N_h \geqq 120$ recorded in the full LST detector. This requirement was introduced in order to eliminate spurious triggers due to random superpositions of beam associated noise in the detector. For this purpose a hardware adder was properly designed and constructed [25].

The trigger rate was 4 Hz. A sizeable fraction, $\simeq 32\%$, was found to be due to spurious triggers, originated by the high level of the radiation associated with the beam, and were discarded. Of the remaining 2.7 Hz, 2.4 were due to CR muons traversing the apparatus which did not trigger the veto. The CR veto inefficiency was measured to be lower than $\sim 5 \cdot 10^{-3}$. Finally ~ 0.3 Hz were due to cosmic neutral particle interactions in the detector.

In order to determine ε_{trig}, a sample of 10^4 $\bar{n}$-annihilation events were generated in the target through a MC. It was found $\varepsilon_{trig} = 77\%$.

The trigger status was continuously monitored and the counting rates were recorded during every experimental run.

The data acquisition system [26] was based on a DEC MicroVax II computer inserted in a local area Vax cluster environment together with 4 workstations to execute on-line monitor, event display and off-line analysis.

The dead time fraction for the trigger system was 1.2% due to the trigger and data acquisition system and 5% due to the veto system.

4 Data analysis

The experiment was taking data from August 1989 to April 1991 when the data taking was ended by the ILL

reactor breakdown. The effective running time was $T=2.4\cdot10^7$ s, the number of useful events was $6.8\cdot10^7$.

The upper limit for the total number of the expected $\bar{n}$-annihilation events, $\bar{N}\leqq300$, was set by making use of the preliminary result $\tau_{n\bar{n}}\geqq10^7$ s [2]. These events had to be selected from several millions of CR neutral interactions. The two types of events were expected however to behave at odds, so to allow very effective selection criteria.

In order to study the CR event frequency and configuration, data were taken during $\sim10^6$ s with the neutron beam off, obtaining a trigger rate for neutral interaction events of 0.3 Hz, in excellent agreement with the trigger rate obtained during the $n\rightleftharpoons\bar{n}$ runs. In addition, the comparison of the CR events produced during beam on and beam off periods provided a detailed analysis of the beam associated noise. The cosmic ray interaction vertices were distributed over the full detector, according to the local matter density. Their energy spectrum was very widespread, peaking at energies lower than 1 GeV and their momenta pointed downward in the apparatus. The candidate $\bar{n}$-annihilation vertices instead were expected in the annihilation target, their energies about 2 GeV and their momenta about zero, the pions going from the inner to the outer SC. Therefore candidate events were required to have

i) vertex inside the annihilation target,
ii) visible energy between 1 and 2 GeV,
iii) energy and momentum isotropically distributed.

These selection criteria were implemented in the analysis in two subsequent phases: software filter and final analysis.

4.1 *Simulation of the annihilation event*

A special MC program was developed for the analysis (MCA) [27]. In this program $\bar{n}$-annihilation events were generated in the target, according to the characteristics of the $\bar{n}$ annihilation in carbon. The tracks of the produced particles were simulated inside the detector, taking into account the particle and the detector properties.

A simple model of internuclear cascade based on experimental data on π interactions in nuclei [28], was able to reproduce the experimental π multiplicity in $\bar{p}$ annihilation in carbon nuclei: 4.5 pions, 2.7 of which charged [29]. Moreover the results of an experimental test, with $\bar{p}$ annihilation at rest in a C target were used. This test was performed at the CERN PS (K23 beam line) [30], with a detector composed of the same elements as those used in this experiment: charged and neutral pion production multiplicity and subsequent interaction probability were measured.

The geometry, the structure and the measured characteristics of the detector were implemented in the MCA through the GEANT code. The streamer tube response to charged tracks was modelled using the measured hit multiplictiy distributions on LST planes, measured with atmospheric muons crossing the apparatus at different incidence angles. In addition the vertex detector as well as the calorimeter detector response to electromagnetic showers, determined by measuring a sample of π^0 produced in the detector, was used in the MCA event simulations [32]. The SC energy threshold and time resolution, experimentally measured, were also included in the MCA.

A sample of 10 000 events simulated by the MCA were translated to a format identical to the experimental one. Moreover randomly distributed hits on LSTs and on SCs, due to the beam associated noise as measured in the experimental events, were properly associated to each MCA event. The MCA events were finally processed through all the filters and analysis programs used for the experimental events.

4.2 *Software filter*

The $6.8\cdot10^7$ triggers went through a software filter [33], where the selection criteria were applied in the sequence described below. This sequence was chosen to minimize the global computer time needed for event selection.

a) The event visible energy. This criterion was chosen with the twofold purpose of discarding most of the CR events: neutral interactions as well as muons passing through the apparatus. In both cases the average energy deposition in the detector was smaller than 1 GeV.

A careful experimental analysis was performed in order to estimate the event visible energy by means of the measurement of N_h: the event number of hits on the LST. Tracks with known deposited energy, as for example throughgoing CR muons or pions stopping in the apparatus having traversed two SC layers, were selected and their N_h was correlated with the corresponding energy. Furthermore, N_h of γ's from π^0 were measured and correlated to their evaluated energy. To this purpose the isolated hits, randomly generated by neutron beam noise, were identified and subtracted. The experimental correlation between N_h and energy was then compared and found to be in very good agreement with the correlation N_h-energy of the pions produced in MCA generated events. Subsequently a relation between E_{vis} and N_h for the events was determined by averaging over the MCA generated events. As a result the relation $E_{\text{vis}}=(185+2.2\,N_h)$ MeV was determined within a 20% accuracy. On this basis, it was decided to select events with $N_h>300$ namely $E_{\text{vis}}>(850\pm170)$ MeV.

Furthermore, the barycenter of hits was determined for each event and events were accepted if they were inside a circle of radius $r=80$ cm, centered in the center of target, in accordance with the fact that for the $\bar{n}$-annihilation events the hit barycenter practically coincided with the event vertex. In addition, events consistent with a single straight track traversing the detector downwards, were identified as crossing muons and discarded. It turned out that 90% of the $6.8\cdot10^7$ collected events did not satisfy these requirements. On the contrary, 85% of the MCA generated events had $N_h>300$ and the hit barycenter in the region chosen, and only 0.7% of them satisfied the single straight track hypothesis.

b) Time of flight. For each particle of each event the times measured in the SCs were considered. SCs signals not associated with charged tracks were disregarded as due to radiation beam associated background. The average value of the inner SCs, $\langle T_{\text{SC}}\rangle_{\text{in}}$, as well as the aver-

age value of the outer SCs, $\langle T_{SC}\rangle_{out}$, were computed. Events were rejected when at least one SC time was 2.5 ns away from the average.

The MCA generated events which satisfied the previous selection criterium were analyzed in the same way and the value of $D=(\langle T_{SC}\rangle_{out}-\langle T_{SC}\rangle_{in})$ was calculated for each event. It was then determined that value D was well inside the region $0<D<5$ ns for all but a 4%. With this requirement 16.4% of the events were retained, with an efficiency for $\bar{n}$-annihilation event detection of 96%.

c) Events vertices. A pattern recognition routine was used to identify the particle tracks of each event and to determine the coordinates of their vertex. Events were retained if they had at least three tracks and vertex inside the region defined by the coordinates $R=(x^2+y^2)^{1/2}<60$ cm, and $|z|<32$ cm ($x=y=z=0$ were the coordinates of the target center).

A subsample of the measured event vertices is shown in Fig. 6.

In order to test the quality of this procedure as well as the efficiency for $\bar{n}$-annihilation detection, the vertices of several thousand experimental and MCA generated events were measured by a physicist with an interactive program and then compared with those provided by the pattern recognition routine. The agreement was good with the exception of a small fraction of events, about 10%, which had one or more particles interacting in the detector or which were incorrectly associated with a crossing particle.

In addition, since the event tracks were expected to be isotropically distributed, events were accepted if their tracks projected in the cross sectional plane orthogonal to the beam axis were contained inside an angle larger than 170°. The event vertex requirements were satisfied by 1.2% of the experimental events, and by 90% of the MCA events.

At the end of the software filter analysis, $1.2\cdot10^4$ events were left, corresponding to $1.8\cdot10^{-4}$ of the original sample. The efficiency of this procedure was $\varepsilon_{filter}=0.72$.

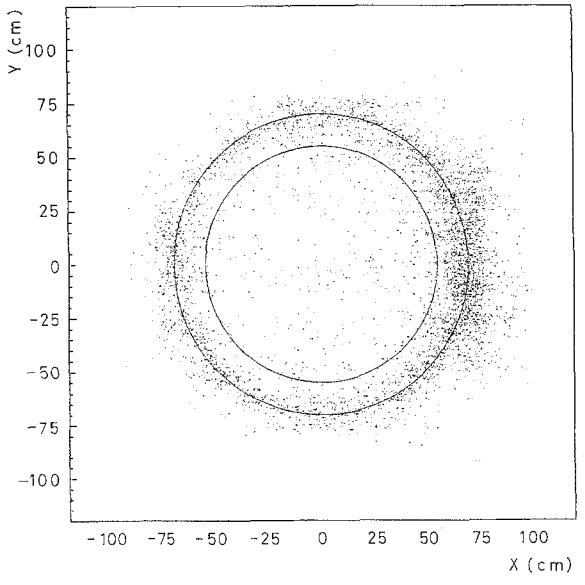

Fig. 6. Vertex distribution in the plane orthogonal to the beam axis of a subsample of reconstructed events

Table 1. Percentages of experimental and simulated events selected by the filter criteria sequentially applied

Filter requirements	% of accepted events	% of accepted Monte Carlo
Energy	10.0	85.0
TOF	16.4	96.0
Vertex	1.2	89.0
Total	0.018	72.0

Table 1 displays the effects of the various criteria on the experimental and on the MCA events.

4.3 Final analysis

The events surviving the filter chain were visually inspected in two independent scannings. 100 MCA generated events were mixed with the $1.2\cdot10^4$ events in order to estimate the scanning efficiency for $\bar{n}$ annihilations, which resulted to be $\varepsilon_{scan}=98\%$.

Most of surviving events were CR muons crossing the apparatus, with an associated electromagnetic activity, or events in which the vertex was incorrectly reconstructed. The scanners were instructed to recognize and reject these events.

After the visual inspection 403 events were left. These events were accurately examined by physicists: particle tracks were reconstructed and the times recorded by PMTs were considered: 68 events, clearly induced by incoming charged CR were disregarded.

The vertices of the 335 remaining events were then reconstructed with an interactive program.

To evaluate the quality of the measurement, a sample of 250 experimental events was measured, chosen in the vicinity of the target, with the vertices on the beam tube, in the region where the tube was isolated from the SC planes. It turned out that the resolution on R, measured in the detector plane orthogonal to the beam axis was ±3.8 cm. The same type of measurement was performed on a sample of 200 MCA events, which had been accepted by the previous selection critieria. They provided a resolution on R of 4.5 cm, in very good agreement with the resolution of the experimental events; furthermore the z coordinate of the 200 MCA events was measured with a resolution of 4.2 cm.

According to these results it was then required that $\bar{n}$-annihilation candidate event vertices satisfy the conditions $R\leqq55$ cm and $|z|\leqq15$ cm.

Only 5, out of the 335 remaining events, satisfied these conditions.

The visible energies of the 5 remaining events were measured directly. The track lengths were measured, π^0 were reconstructed and then the event energies were properly evaluated. Three events, which turned out to have a visible energy $E_{vis}<800$ MeV, were disregarded. The remaining 2 events were rejected on the basis of the isotropy requirements. The barycenter of their hits lay far below their vertices, a characteristic of the CR interactions. The MCA $\bar{n}$-annihilation event sample, satisfying the previous requirements, showed that the distribution of the difference y_{vb} between the vertical position of vertex and

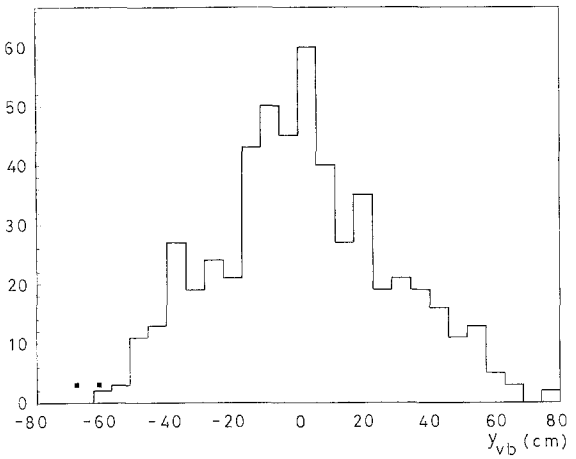

Fig. 7. Distribution of the difference between the vertical coordinates of vertices and the barycenter of the hits for MCA events (histogram) and the two experimental events (black squares)

hit barycenter was peaking at 0 and greater than -60 cm, see Fig. 7. The y_{vb} values of the two remaining events from the final sample were measured and found $y_{vb} < -60$ cm. The events were then discarded as due to CR interactions.

250 MCA generated events, surviving the previously defined filter, were processed together with the 335 experimental events in order to determine the efficiency of this procedure for the detection of $\bar{n}$-annihilation events, which resulted to be 97%.

Thus the overall efficiency ε for $\bar{n}$ annihilation detection was:

$$\varepsilon = \varepsilon_{\text{trig}} \cdot \varepsilon_{\text{filter}} \cdot \varepsilon_{\text{analysis}}$$

$$= 0.770 \cdot 0.72 \cdot 0.95 = 0.52 \pm 0.02 .$$

5 The limit on $\tau_{n\bar{n}}$

Table 2 summarizes the experimental data.

No candidate $\bar{n}$-annihilation was found in $2.4 \cdot 10^7$ s running time, and the lower limit for $\tau_{n\bar{n}}$

$$\tau_{n\bar{n}} = \left(\frac{IT(1-d)\langle \eta \rangle \varepsilon \langle t^2 \rangle}{\bar{N}} \right)^{1/2} \geqq 0.86 \cdot 10^8 \text{ s} \qquad (10)$$

was set at 90% C.L..

Acknowledgements. We thank the directors and staff at the Institute Laue-Langevin in Grenoble for their support during the experiment. The experiment would not have been possible without the skilled technical assistance from our laboratories. We express our gratitude to all technicians from our universities, who contributed so much to the success of the experiment. This work has been funded jointly by the German Federal Minister for Research and Technology (BMFT) under contract number 06HD9831, the Institute Laue-Langevin in Grenoble and the Istituto Nazionale di Fisica Nucleare, Italy.

Table 2. Experimental data

I, neutron intensity	$(1.25 \pm 0.06) \cdot 10^{11}$ n s^{-1}
$\langle t^2 \rangle^{1/2}$, neutron "quasi free" propagation time	0.109 ± 0.002 s
T, effective running time	$2.40 \cdot 10^7$ s
d, experimental dead time	6.2%
$\langle \eta \rangle$, "quasi free" condition efficiency	0.984 ± 0.003
$\varepsilon_{\text{trig}}$, trigger efficiency	0.77
$\varepsilon_{\text{filter}}$, filter efficiency	0.72
$\varepsilon_{\text{analysis}}$, analysis efficiency	0.95
ε_2, $\bar{n}$ detection efficiency	0.52 ± 0.02
$\bar{N}$, number of candidate events	0 (≤ 2.3 at 90% C.L.)

References

1. For a review, see: R.N. Mohapatra: Nucl. Instrum. Methods A284 (1989) 1
2. M. Baldo-Ceolin et al.: Phys. Lett. 236B (1990) 95
3. G. Fidecaro et al.: Phys. Lett. 156B (1985) 122
4. G. Bressi et al.: Z. Phys. C43 (1989) 175; G. Bressi et al.: Nuovo Cimento 103A (1990) 731
5. K. Nakamura: Proceedings of the 25th International Conference on High Energy Physics, Singapore (1990), p. 281, and bibliography therein
6. C.B. Dover, A. Gal., J.M. Richard: Phys. Rev. C31 (1985) 1423; W.M. Alberico, A. De Pace, M. Pignone: Nucl. Phys. A523 (1991) 488 and bibliography therein
7. P.K. Kabir: Phys. Rev. Lett. 51 (1983) 231; J. Baseq, L. Wolfenstein: Nucl. Phys. B224 (1983) 21; P.K. Kabir, J. Noble: Univ. of Virginia - Preprint (1989)
8. M. Baldo-Ceolin: Proceedings of the Conference on Astrophysics and Elementary Particles: Common Problems, Accademia Nazionale dei Lincei, Roma (1980) 251; R.E. Marshak, R.N. Mohapatra: Phys. Lett. 94B (1980) 183
9. P. Ageron: Nucl. Instrum. Methods A284 (1989) 197
10. T. Bitter et al.: Nucl. Instrum. Methods A321 (1992) 284
11. A. Guglielmi: Progress in Nuclear Energy, Vol. 24, (1990) 429; T. Bitter: Ph.D. thesis, Heidelberg, 1989
12. See e.g.: Physics at LEAR in the ACOL era, U. Gastaldi et al. (eds.). Gif-sur-Yvette: Editions Frontieres 1985
13. F. Eisert et al.: Nucl. Instrum. Methods A313 (1992) 477
14. A. Guglielmi: Nucl. Instrum. Methods A325 (1993) 241
15. G. Costa, P. Kabir: Phys. Rev. D28 (1983) 667
16. T. Bitter et al.: Nucl. Instrum. Methods A309 (1991) 521; W. Lippert: Ph.D. thesis, Heidelberg, 1990
17. U. Kinkel: Z. Phys. C54 (1992) 573
18. T. Bitter, D. Dubbers: Nucl. Instrum. Methods A239 (1985) 461; U. Schmidt et al.: Nucl. Instrum. Methods A320 (1992) 569; P. El-Muzeini: Ph.D. thesis, Heidelberg, 1991
19. E. Iarocci: Nucl. Instrum. Methods A217 (1983) 30
20. A. Cavestro et al.: Nucl. Instrum. Methods A305 (1991) 488
21. M. Baldo-Ceolin et al.: Nuovo Cimento A105 (1992) 1679
22. A. Cavestro et al.: Nucl. Instrum. Methods A313 (1992) 571
23. G.L. Raselli: Ph.D. thesis, Pavia, 1991
24. M. Baldo-Ceolin et al.: IEEE Trans. Nucl. Sci. 38-2 (1991) 471
25. A. Cavestro et al.: DFPD 92/EI/55 (1992)
26. M. Mezzetto: Ph.D. thesis, Padova, 1986
27. D. Gibin: Ph.D. thesis, Padova, 1989
28. D.A. Sparrow, M.M. Sternheim: Phys. Rev. C10 (1974) 2215; D.A. Sparrow: Phys. Rev. Lett. 44 (1980) 625
29. L.E. Agnew et al.: Phys. Rev. D118 (1960) 1371
30. D. Gibin, M. Mezzetto, M. Rigano: $N\bar{N}$ Internal Note 7, 1984
31. R. Brun et al.: Geant 3, CERN DD/EE/84-1, Geneva 1986
32. E. Brunello: Degree Thesis, Padova 1990; M. Genoni: Ph.D. thesis, Pavia, 1991
33. D. Gibin, M. Mezzetto: $N\bar{N}$ Internal Note PD-92-1